Research Article

Cancer Immunology Research

SLAMF6 as a Regulator of Exhausted CD8$^+$ T Cells in Cancer

Burcu Yigit[1], Ninghai Wang[1], Elisa ten Hacken[2], Shih-Shih Chen[3], Atul K. Bhan[4], Abel Suarez-Fueyo[5], Eri Katsuyama[5], George C. Tsokos[5], Nicholas Chiorazzi[3], Catherine J. Wu[2], Jan A. Burger[6], Roland W. Herzog[7], Pablo Engel[6,8], and Cox Terhorst[1]

Abstract

The tumor microenvironment in leukemia and solid tumors induces a shift of activated CD8$^+$ cytotoxic T cells to an exhausted state, characterized by loss of proliferative capacity and impaired immunologic synapse formation. Efficient strategies and targets need to be identified to overcome T-cell exhaustion and further improve overall responses in the clinic. Here, we took advantage of the Eμ-TCL1 chronic lymphocytic leukemia (CLL) and B16 melanoma mouse models to assess the role of the homophilic cell-surface receptor SLAMF6 as an immune-checkpoint regulator. The transfer of SLAMF6$^+$ Eμ-TCL1 cells into SLAMF6$^{-/-}$ recipients, in contrast to wild-type (WT) recipients, significantly induced expansion of a PD-1$^+$ subpopulation among CD3$^+$CD44$^+$CD8$^+$ T cells, which had impaired cytotoxic functions. Conversely, administering anti-SLAMF6 significantly reduced the leukemic burden in Eμ-TCL1 recipient WT mice concomitantly with a loss of PD-1$^+$CD3$^+$CD44$^+$CD8$^+$ T cells with significantly increased effector functions. Anti-SLAMF6 significantly reduced leukemic burden in the peritoneal cavity, a niche where antibody-dependent cellular cytotoxicity (ADCC) is impaired, possibly through activation of CD8$^+$ T cells. Targeting of SLAMF6 affected tumor growth not only in B cell–related leukemia and lymphomas but also in nonhematopoietic tumors such as B16 melanoma, where SLAMF6 is not expressed. *In vitro* exhausted CD8$^+$ T cells showed increased degranulation when anti-human SLAMF6 was added in culture. Taken together, anti-SLAMF6 both effectively corrected CD8$^+$ T-cell dysfunction and had a direct effect on tumor progression. The outcomes of our studies suggest that targeting SLAMF6 is a potential therapeutic strategy.

Introduction

T-cell exhaustion, associated with the inability to mount successful antitumor immune responses, has increasingly become a target for immunotherapy. Programmed cell death 1 protein (PD-1, CD279) is well characterized as an inhibitory receptor that is upregulated during immune evasion (1–5). PD-1 expression under physiologic conditions controls the magnitude of T-cell effector functions upon activation (6). Within the tumor microenvironment, however, overexpression of the PD-1 ligand, PD-L1, on the surface of tumor cells increases the likelihood of its binding to PD-1 on T cells, which, in turn, suppresses T-cell effector functions (6, 7). PD-1 expression is also associated with an exhausted state of T cells. Blocking the PD-1/PD-L1 axis has been demonstrated to be an effective way to remove the break on these otherwise suppressed T cells, restoring their cytotoxic capacity in the setting of advanced solid tumors, as well as in leukemias (8, 9).

Signaling lymphocyte activation molecule family 6, SLAMF6 (CD352, Ly108, NTB-A), is a homophilic cell-surface receptor, belonging to the immunoglobulin superfamily (10, 11). SLAMF6 is a type I transmembrane protein with two extracellular immunoglobin (Ig)-like domains and three cytoplasmic tyrosine-based signaling motifs, one of which is immunoreceptor tyrosine-based switch motif (ITSM; refs. 10, 12). The SLAMF6 receptor is expressed on the surface of a wide variety of hematopoietic cells, e.g., T, B, and natural killer (NK) cells (expression restricted to human), and interactions on different cell types allow for diverse immunomodulatory functions, some of which include adhesion, innate T-lymphocyte development, neutrophil function, and NK and CD8$^+$ T cell–mediated cytotoxicity (13–22). Upon phosphorylation of the immunoreceptor, the two ITSMs, the SH2 domain-containing T- and NK cell adaptor SLAM-associated

[1]Division of Immunology, Beth Israel Deaconess Medical Center, Harvard Medical School, Boston, Massachusetts. [2]Department of Medical Oncology, Dana-Farber Cancer Institute, Boston, Massachusetts. [3]Karches Center for Oncology Research, The Feinstein Institute for Medical Research, Manhasset, New York. [4]Department of Pathology, Massachusetts General Hospital, Harvard Medical School, Boston, Massachusetts. [5]Division of Rheumatology, Beth Israel Deaconess Medical Center, Harvard Medical School, Boston, Massachusetts. [6]Department of Leukemia, The University of Texas MD Anderson Cancer Center, Houston, Texas. [7]Herman B Wells Center for Pediatric Research, Indiana University School of Medicine, Indianapolis, Indiana. [8]Immunology Unit, Department of Cell Biology, Immunology and Neurosciences, Medical School, University of Barcelona, Barcelona, Spain.

Note: Supplementary data for this article are available at Cancer Immunology Research Online (http://cancerimmunolres.aacrjournals.org/).

B. Yigit and N. Wang contributed equally to this article.

Corresponding Authors: Burcu Yigit, Beth Israel Deaconess Medical Center, Harvard Medical School, 3 Blackfan Circle, Center for Life Sciences, Room CLS 928, Boston, MA 02115. Phone: 617-735-4136; E-mail: byigit@bidmc.harvard.edu; and Cox Terhorst, Beth Israel Deaconess Medical Center, Harvard Medical School, 3 Blackfan Circle, Center for Life Sciences, Room CLS 938, Boston, MA 02115. Phone: 617-735-4157; Fax: 617-735-4140; E-mail: cterhors@bidmc.harvard.edu

Cancer Immunol Res 2019;7:1485–96

doi: 10.1158/2326-6066.CIR-18-0664

protein (SAP) is recruited to the SLAMF6 cytoplasmic tail (12, 21, 23). Upon engagement of SLAMF6, the ensuing signaling induces both cooperation between T follicular helper cells and germinal center B cells (18), as well as interactions between cytotoxic T-cell and B-cell targets (23). This process is dependent upon the presence of SAP. By contrast, in the absence of SAP, SLAMF6 negatively regulates both processes by recruiting the tyrosine phosphatases SHP1 and SHP2 to its cytoplasmic tail.

Because B cells do not express SAP, we previously hypothesized that triggering SLAMF6 would negatively regulate B-cell responses. Indeed, the monoclonal antibodies 13G3 and 330 directed against mouse SLAMF6 (24) react with TCL1-192 cells, a $CD5^+$ chronic lymphocytic leukemia (CLL) B-cell clone that had been transferred into SCID mice (25, 26). One injection of the antibody limits the expansion of TCL1-192 due to antibody-dependent cellular cytotoxicity (ADCC) and downregulation of B-cell receptor (BCR) signaling (26). Based on these observations, we then hypothesized that antibodies directed against SLAMF6 should also affect the immunomodulatory action of cytotoxic T cells that respond to Eμ-TCL1 CLL cells. Here, we showed that anti-SLAMF6 increases the $CD8^+$ T-cell responses to CLL, resulting in a significantly reduced proportion of exhausted cytotoxic T lymphocytes (CTL). We also demonstrated that anti-SLAMF6 arms $CD8^+$ T cells in not only B-cell leukemias but also non-hematopoietic solid tumors such as B16 melanoma, where the tumors do not express SLAMF6. Thus, anti-SLAMF6 increases CTL responses to and affects the expansion of both the leukemic cells and solid tumors.

Materials and Methods

Mice

C57BL/6J (B6) wild-type (WT) mice were obtained from The Jackson Laboratory. Eμ-TCL1 mice (25) were kindly provided by Dr. Amy Johnson (Ohio State University, Columbus, OH). $SLAMF6^{-/-}$ B6 mice were generated from Bruce4 ES cells (27). $SAP^{-/-}$ mice were generated as described elsewhere (28). All animals were maintained under specific pathogen-free conditions at the Beth Israel Deaconess Medical Center (BIDMC; Boston, MA) animal facility. Experiments were performed in accordance with the guidelines and with the approval of the institutional animal care and use committee (IACUC) at BIDMC.

CLL cells

Frozen peripheral blood mononuclear cells (PBMC) provided by Dr. Jan Burger at The University of Texas MD Anderson Cancer Center (Houston, TX) were used for all experiments. Information on patient samples is provided in Supplementary Table S1. Written patient consent for samples used in this study was obtained in accordance with the Declaration of Helsinki on protocols that were approved by the institutional review board at the BIDMC and at The University of Texas MD Anderson Cancer Center.

In vitro stimulation of human CLL cells

Briefly, frozen CLL PBMCs were thawed, washed, and resuspended in RPMI-1640 (Gibco) + 10% fetal bovine serum (FBS) + 1× penicillin/streptomycin (Gibco) + 1× L-glutamine (Gibco). This same medium was used in all *in vitro* experiments. Fifty to 100,000 cells were either left unstimulated or stimulated with goat anti-human $F(ab')_2$ IgM (20 μg/mL; MP Biomedical) alone, together with 1 μmol/L ibrutinib (ChemieTek) or anti-human SLAMF6 (10 μg/mL; BioLegend), or in combination with both. Cells were cultured for 24 and 48 hours, and viability was determined by Annexin V/propidium iodide (PI; BioLegend) staining by BD LSRII flow cytometry.

Degranulation was assessed in a 96-well U-bottom plate coated with anti-CD3 (5 μg/mL; OKT3, Bio X Cell) and anti-CD28 (5 μg/mL; CD28.2, BioLegend). Some wells were also coated with anti-human SLAMF6 (5 μg/mL; NT-7, BioLegend) or mouse IgG2b isotype control (5 μg/mL, BioLegend). CLL B cells were isolated from PBMCs by using CD19 microbeads (Miltenyi Biotec), and the remaining cells were plated as 2.5×10^5 cells/well. Cells were then stimulated in the presence of 2 μL of anti-CD107a. After 30 minutes at 37°C and 5% CO_2, brefeldin A (1:1,000; BD Biosciences) was added, and incubation continued for 4 hours. Cells were washed twice with cold PBS and stained for extracellular markers for 30 minutes at 4°C in FACS-staining buffer [PBS, 1% BSA (Sigma-Aldrich), 2 mmol/L EDTA]. After two washes, cells were resuspended in FACS-staining buffer and analyzed by using a Cytoflex cytometer (Beckman Coulter). Data were analyzed by using Cytexpert software (Beckman Coulter). Antibodies used for these experiments are listed in Supplementary Table S1.

In vitro T-cell exhaustion

Fresh PBMCs were obtained from 5 healthy donors who provided written consent for the study (BIDMC). The Lymphoprep separation kit (STEMCELL Technologies) was used to isolate PBMCs from whole blood. Cells were then washed with PBS and counted. Ninety-six–well plates were coated with anti-CD3 and anti-CD28 (1 μg/mL each), and cells were plated at 2.5×10^5 cells/well in RPMI medium. Every 2 days, cells were resuspended, washed, and transferred to a new 96-well plate coated with the same concentration of anti-CD3 and anti-CD28. On day 8, cells were collected and checked for exhaustion markers via flow cytometry, and degranulation assays were performed with isotype or anti-human SLAMF6 (5 μg/mL), as explained above.

The *in vivo* Eμ-TCL1 adoptive transfer model

Fresh or frozen splenocytes (15×10^6–20×10^6 per mouse) from 12- to 14-month-old leukemic Eμ-TCL1 mice were injected intraperitoneally (i.p.) into 8- to 12-week-old B6 WT or $SLAMF6^{-/-}$ recipients. Mice were irradiated at 400 Rad prior to leukemic transplantation. For experiments involving anti-SLAMF6 or isotype injections, mice were bled via tail vein biweekly for 4 weeks after transfer. When leukemic burden (percentage of $CD19^+CD5^+$) reached 20% to 40% in blood, mice were randomized and injected i.p. with 200 μg/mouse anti-mouse SLAMF6 (13G3; ref. 18; anti-SLAMF6 is an agonistic antibody that can induce positive or negative signaling depending on the recruitment of its adaptor SAP or SHP1/2 on its cytoplasmic tail) or mIgG2a isotype control (clone C1.8; Bio X Cell; $n = 16$ for each group). Mice were injected a total of 3 times, biweekly, and were euthanized 1 week after the third injection. Cells from the peritoneal cavity (PerC) were collected by flushing 10 mL PBS + 2% FBS and subsequent drawing of the fluid from the PerC. Bone marrow cells were flushed from the femurs with 5 mL PBS + 2% FBS. Single-cell suspensions were prepared from spleen, and red blood cells (RBC) were removed by RBC lysis buffer (Sigma). Serum was obtained by centrifugation at 8,000 × *g* for 10 minutes at room temperature (RT).

B16-OVA melanoma

The B16-OVA cells were kindly donated and authenticated by Dr. James Mier (Division of Hematology/Oncology at the BIDMC). The cells were cultured in RPMI medium with 10% FBS, and during the expansion phase, 10^5 B16-OVA cells were injected subcutaneously into each B6 WT mouse. Eight days after injection, 100 μg/mouse anti-SLAMF6 or isotype control was i.p. injected, and tumor volume was monitored daily by measuring 3 diameters using a caliper. On day 15, mice were euthanized, solid tumors were extracted, and lymphocytes were isolated by digesting the tumors with collagenase IV (Gibco) for 30 minutes at 37°C (29).

Flow cytometry

Antibodies used for flow cytometry are listed in Supplementary Table S2. Surface staining was done by first incubation with 20% rabbit serum (Rockland Immunochemicals) + Fc block (BioLegend) for 10 minutes at RT, and the prepared antibody cocktails were incubated with cells for 30 minutes at 4°C. Samples were washed twice with FACS buffer (PBS + 2% FBS) and analyzed on a five-laser BD LSRII analyzer (BD Biosciences). Viable cells were gated as diaminidino-2-phenylindole (DAPI; Thermo Fisher) negative, and doublets were excluded. Results were analyzed by FlowJo software.

Identification of cytotoxic $CD8^+$ T cells

Fresh splenocytes isolated from mice were cultured with phorbol myristate acetate (PMA; 50 ng/mL) and ionomycin (Sigma-Aldrich; 1 μg/mL) for 4 hours in the presence of brefeldin A (1 μL/mL) at 37°C with 5% CO_2. After 4 hours, cells were washed twice with PBS, and cells were stained for CD3 and CD8, as mentioned in flow cytometry section. Next, cells were fixed and permeabilized using BD Cytofix/Cytoperm kit, according to the manufacturer's protocol, and intracellular staining for granzyme B, IFNγ, and IL2 was performed. For CD107a staining, the antibody was added to the culture in the beginning for cell-surface staining of CD107a upon degranulation, as described above.

Histology

Liver sections were harvested at the end of the experiment and were fixed in 10% formalin and stained with hematoxylin and eosin (H&E) at the BIDMC histology core. Assessment was done by Dr. Atul Bahn at Massachusetts General Hospital (Boston, MA).

Statistical analysis

Statistics for normally distributed mouse data sets were done by an unpaired Student *t* test, whereas for nonnormally distributed sets, a two-sided Mann–Whitney *U* test was used. For human CLL data, a nonparametric Wilcoxon signed-rank test was used. Values reported as mean ± SD, and analyses were carried out using GraphPad Prism.

Results

Exhausted $PD1^+CD8^+$ T cells in $SLAMF6^{-/-}$ B6 mice responding to TCL1-CLL cells

To assess the role of SLAMF6 on the expansion of murine CLL cells, we transferred $SLAMF6^+$ Eμ-TCL1 into irradiated $SLAMF6^{-/-}$ or WT B6 mice. When recipient mice were euthanized 35 days after transfer, no significant difference in the spleen size or total number of splenocytes was detected (Supplementary Fig. S1A and S1B). As judged by the percentage of $CD19^+CD5^+$ TCL1 cells among lymphocytes in spleen, blood, PerC, and bone marrow, leukemic infiltration was unaffected by the absence of SLAMF6 interactions in the tumor microenvironment (Supplementary Fig. S1C). No difference in the percentages of $CD3^+$ T cells (CD3: 6.1% ± 0.2% vs. 7.5% ± 0.6%) was observed between the two strains of recipient mice (Supplementary Fig. S1D). SLAMF6 was expressed at comparable levels among T-cell subsets from WT recipients (Supplementary Fig. S2A and S2B).

The spleens of $SLAMF6^{-/-}$ recipients harbored significantly increased numbers ($1.2 \pm 0.4 \times 10^6$ vs. $1.7 \pm 0.2 \times 10^5$, $P < 0.0001$) and proportions (4.5 ± 0.7 vs. 13.1 ± 3, $P = 0.0019$) of $PD\text{-}1^+CD3^+CD44^+CD8^+$ antigen-experienced T cells compared with WT mice (Fig. 1A). Because this suggested that the presence of SLAMF6 could negatively regulate $CD8^+$ T-cell exhaustion, we assessed relevant effector functions. The CTL effector functions of $CD8^+$ T cells isolated from $SLAMF6^{-/-}$ recipients were impaired, as measured by CD107a [23.2% ± 3.3% vs. 18.5% ± 0.7%, not significant (ns)], and intracellular granzyme B (41.9% ± 2.5% vs. 28% ± 1.7%, $P = 0.002$) and IFNγ (46.5% ± 0.9% vs. 38.2% ± 1.8%, $P = 0.003$), whereas IL2 production remained unchanged (Fig. 1B and C). An increase in $CD8^+$ T cells was reflected by a diminished $CD4^+/CD8^+$ ratio in $SLAMF6^{-/-}$ mice as compared with the WT recipients ($CD4^+/CD8^+$ ratio 1.7 ± 0.12 vs. 2.2 ± 0.18, $P = 0.04$; Fig. 1D). Within $CD4^+$ and $CD8^+$ T-cell subsets, there was no significant shift in naïve ($CD62L^+CD44^-$) and effector/memory ($CD62L^-CD44^+$/$CD62L^+CD44^+$) subsets (Fig. 1E and F).

It is well recognized that in T cells, SAP is recruited to the cytoplasmic tail of SLAMF6 upon SLAMF6–SLAMF6 ligation, followed by initiation of a SLAMF6-related signaling network (23). To test whether SAP signaling was essential for expansion of exhausted $CD8^+$ T cells, we transferred TCL1 cells into irradiated WT and $SAP^{-/-}$ mice. We found no changes in leukemic burden (Supplementary Fig. S3A) or in the abundance of exhausted T cells in the absence of SAP (Supplementary Fig. S3B–S3D), suggesting that the $PD\text{-}1^+CD8^+$ response to TCL1 is SAP independent. Taken together, these findings suggest that expression and signaling through SLAMF6 negatively controls expansion of $PD\text{-}1^+CD44^+CD8^+$ T cells and subsequent T-cell exhaustion in recipients of Eμ-TCL1 CLL cells.

Anti-SLAMF6 limits expansion of adoptively transferred Eμ-TCL1 CLL cells

To evaluate whether anti-SLAMF6–induced signaling would have an effect on T-cell responses and leukemic expansion, we transferred tumor-bearing splenocytes from Eμ-TCL1 mice into WT mice. When TCL1 cell infiltration in the blood approached 20% to 40%, mice were randomized into 1 of 2 groups to receive once a week i.p. anti-SLAMF6 or IgG2a isotype control (Fig. 2A). One week after the third injection, the recipient mice were sacrificed and analyzed for expansion of the transferred Eμ-TCL1 CLL cells. Spleen weight and the total number of splenocytes of anti-SLAMF6–injected recipient mice were significantly reduced compared with isotype control mice (Fig. 2B and C, left; spleen weight 0.95 ± 0.04 vs. 0.38 ± 0.1 g, $P = 0.003$; total splenocytes $6.1 \pm 1.03 \times 10^8$ vs. $0.74 \pm 0.16 \times 10^8$, $P < 0.0001$). Leukemic cell infiltration in the spleen was also significantly reduced, as judged by the percentage of $CD19^+CD5^+$ lymphocytes (79.7% ± 1.7% vs. 37.3% ± 5.1%, $P < 0.0001$; Fig. 2C, right). Consistent with this,

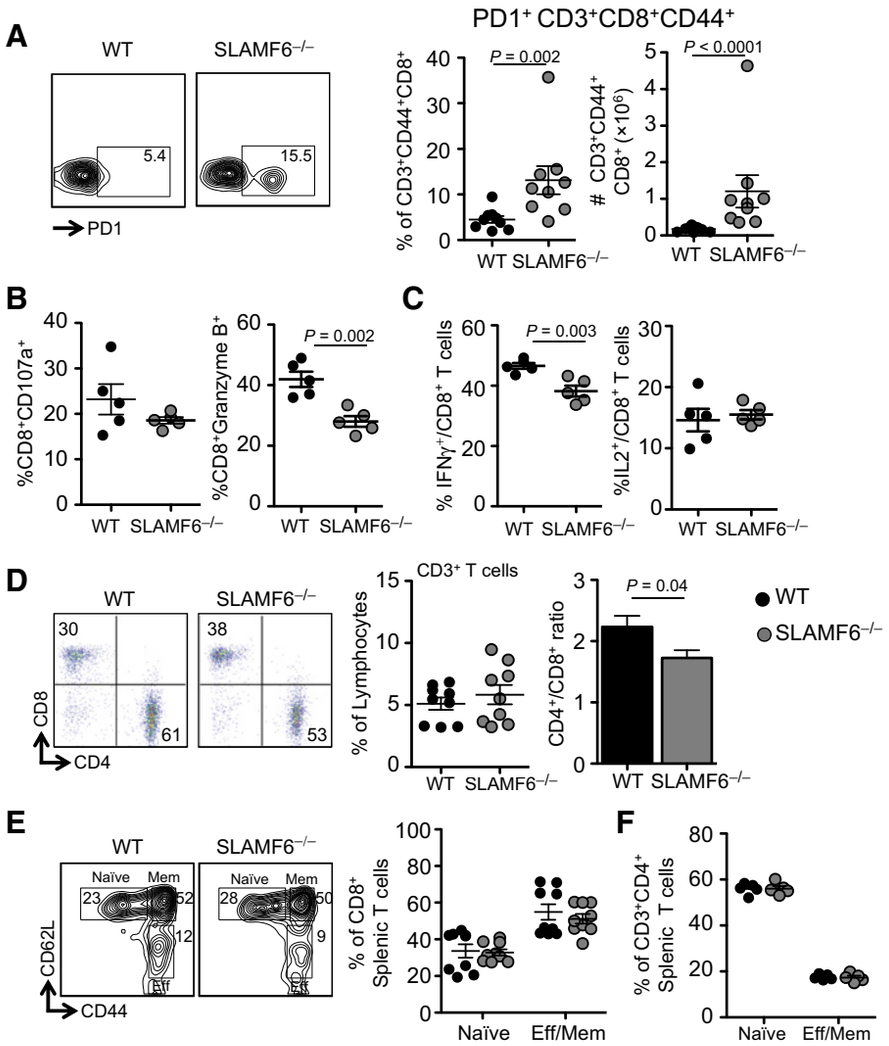

Figure 1.

Expansion of TCL1 cells upon transfer into SLAMF6$^{-/-}$ mice coincides with reduced effector functions and increased exhaustion of CD8$^+$ T cells. Splenocytes from Eμ-TCL1 mice (15–20 × 10^6) were transferred into irradiated (4 Gy) WT ($n = 9$) or SLAMF6$^{-/-}$ ($n = 9$) mice, and after 35 days, the recipient mice were sacrificed for analysis by flow cytometry. **A,** Left, representative plots of PD1$^+$CD3$^+$CD44$^+$CD8$^+$ T cells from the spleen of WT and SLAMF6$^{-/-}$ recipient mice. Right, Percentage and numbers of PD1$^+$CD3$^+$CD44$^+$CD8$^+$ T cells from the spleen. **B,** Fresh total splenocytes from WT and SLAMF6$^{-/-}$–injected mice were cultured with PMA/ionomycin for 4 hours in the presence of brefeldin A. After cell-surface staining with CD3 and CD8, cells were fixed and permeabilized for intracellular staining. CD107a antibody was added to the culture in the beginning. CD107a and granzyme B were a measure of cytotoxic capacity of CD8$^+$ T cells from WT and SLAMF6$^{-/-}$. **C,** IFNγ and IL2 as a measure of effector function of CD8$^+$ T cells in WT vs. SLAMF6$^{-/-}$ groups. **D,** Splenocytes were stained for CD3, CD4, CD8, CD44, and CD62L. Dead cells were excluded as DAPI negative. CD3$^+$, CD3$^+$CD4$^+$, and CD3$^+$CD8$^+$ T-cell percentages in the spleen were compared between WT and SLAMF6$^{-/-}$ mice. **E,** Naïve (CD62L$^+$CD44$^-$) and effector/memory (Eff/Mem; CD62L$^-$CD44$^+$, CD62L$^+$CD44$^+$) subsets as a percentage of CD3$^+$CD8$^+$ T cells in the spleen of WT and SLAMF6$^{-/-}$ mice. **F,** Naïve and effector/memory (Eff/Mem) subsets as a percentage of CD3$^+$CD4$^+$ T cells in the spleen of WT and SLAMF6$^{-/-}$ mice. The data from two independent experiments were pooled. Statistical analyses used the two-sided Mann–Whitney *U* test. All graphs depict the mean ± SD. *P* values are as shown.

anti-SLAMF6–treated recipient mice exhibited a significantly reduced number of TCL1 cells in the blood (73.4% ± 2.3% vs. 38.5% ± 3.8%, $P < 0.0001$) and infiltrating the bone marrow (5.5% ± 1.3% vs. 0.9% ± 0.1%, $P < 0.0001$; Fig. 2D). Administering anti-SLAMF6, as judged by H&E staining, also diminished tumor infiltration in the liver (Fig. 2E). Eμ-TCL1 CLL cells in the spleen and blood of anti-SLAMF6–injected mice appeared significantly more proapoptotic compared with isotype-injected mice, as measured by the percentage of Annexin V$^+$ TCL1 cells (Fig. 2F). We concluded that leukemic cell expansion and viability were significantly reduced by administering anti-SLAMF6 to Eμ-TCL1 CLL cell–bearing B6 mice.

Anti-SLAMF6 reduces the number of exhausted CD8$^+$ T cells

Administering anti-SLAMF6 to Eμ-TCL1 CLL–bearing WT mice caused a shift among splenic CD8$^+$ T cells from naïve (CD62L$^+$CD44$^-$) to antigen-experienced effector memory (eff/mem; CD62L$^+$CD44$^+$) phenotype (naïve 30.5% ± 4.1% vs.

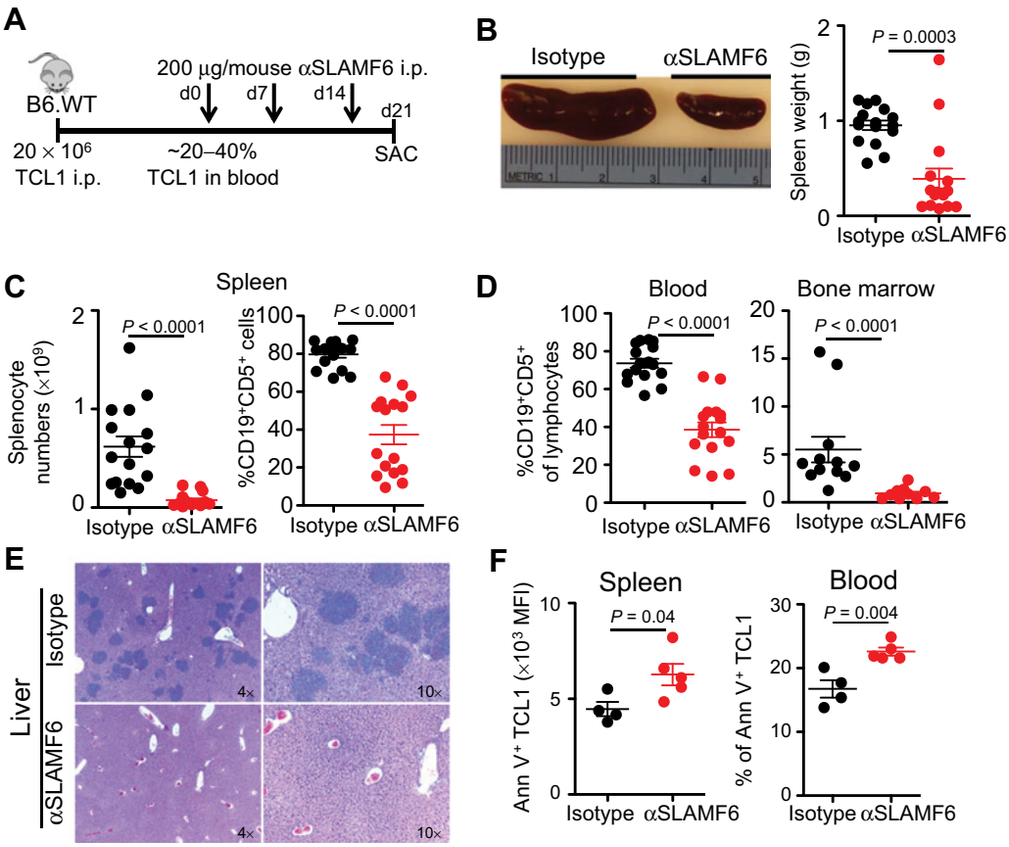

Figure 2.

Injection of mouse anti-mouse-SLAMF6 effectively limits *in vivo* expansion of TCL1 CLL cells in WT (B6) mice. Splenocytes (15×10^6–20×10^6) isolated from Eμ-TCL1 mice were transplanted into WT (B6) mice. When the leukemic burden reached 20% to 40% in the blood, anti-mouse-SLAMF6 IgG (13G3; 200 μg/mouse; $n = 16$) or mouse isotype (IgG2a) control ($n = 16$) was injected. After a total of 3 biweekly injections, mice were euthanized and analyzed, as schematically outlined in **A**. **B,** Representative spleen pictures and spleen weights. **C,** Total number of splenocytes and leukemic cell infiltration as judged by the percentage of $CD19^+CD5^+$ TCL1 cells in the spleen of anti-SLAMF6–injected mice compared with isotype-injected mice. **D,** Percentages of TCL1 cells ($CD19^+CD5^+$) in blood and bone marrow between isotype- and anti-SLAMF6–injected groups. **E,** Representative H&E staining from liver of isotype- and anti-SLAMF6–injected mice. **F,** TCL1 cells isolated from spleen and blood of the anti-SLAMF6–injected group ($n = 5$) to compare apoptosis [percentage of Annexin V^+ (Ann V^+)] to TCL1 cells from the isotype-injected group ($n = 4$). The data obtained in four independent experiments were pooled. The two-sided Mann–Whitney *U* test was used for statistical analysis. All graphs depict mean ± SD. *P* values are as shown.

14.5% ± 3.1%, $P = 0.02$; eff/mem 45% ± 5% vs. 64.8% ± 4.3%, $P = 0.02$; Fig. 3A). This shift in $CD8^+$ T-cell subsets was also observed in the blood (naïve 30.6 ± 3.7% vs. 8.9% ± 2.6%, $P = 0.0008$; eff/mem 54.9% ± 4.5% vs. 80.8% ± 3.9%, $P = 0.001$; Fig. 3B). This increase in the percentage of $CD8^+$ T cells resulted in an increased proportion of $CD3^+$ T cells in the spleen and blood (spleen: 6.6 ± 0.7 vs. 15.3 ± 2.3%, $P = 0.0002$; blood: 7.6 ± 0.9 vs. 17.4%, $P = 0.01$) of anti-SLAMF6–treated tumor recipients (Fig. 3C). This was also reflected in a significantly reduced $CD4^+/CD8^+$ ratio in the spleen of anti-SLAMF6–injected mice (spleen: 1.18 ± 0.1 vs. 0.74 ± 0.17, $P = 0.04$), but not in the blood (blood: 0.68 ± 0.06 vs. 0.61 ± 0.2; Fig. 3D). $CD4^+$ T-cell subsets, i.e., $CD62L^+CD44^-$ or $CD62L^+CD44^+$, were not affected by the anti-SLAMF6 (Supplementary Fig. S4).

Because exhausted $CD8^+$ T cells display a loss of effector function in CLL patients (1), we further analyzed the *in vivo* effect of anti-SLAMF6 on $CD8^+$ T-cell exhaustion. The percentage of activated $CD3^+CD44^+CD8^+$ T cells in the spleen that expressed the well-known marker PD-1 in the anti-SLAMF6–injected group during the response to TCL1 cells was significantly lower compared with that in isotype control mice (3.1% ± 0.5% vs. 11.7 ± 1.6, $P = 0.0002$; Fig. 4A, left), and the absolute number of $PD1^+CD3^+CD44^+CD8^+$ T cells was also reduced in the spleen (0.1 ± 0.03 vs. 0.6 ± 0.1 × 10^6, $P = 0.0003$; Fig. 4A, right). This effect of anti-SLAMF6 was also observed in the blood (5% ± 1% vs. 11.1% ± 1.2%, $P = 0.001$; Fig. 4B). In addition to PD-1, the proportion of $CD3^+CD44^+CD8^+$ T cells expressing additional markers of exhaustion, CD160, LAG3, and KLRG1, was also significantly reduced in the spleen after the injection of anti-SLAMF6 (Fig. 4C).

To test whether the phenotypical changes in the exhausted $CD8^+$ T-cell compartment of anti-SLAMF6–injected mice correlated with an increase in effector functions, splenocytes isolated from anti-SLAMF6–injected mice were *in vitro* stimulated with PMA/ionomycin in the presence of brefeldin A for 4 hours. Intracellular staining of $CD8^+$ T cells showed significantly increased lysosomal CD107a (6.7% ± 0.3% vs. 8.8% ± 0.50%, $P = 0.003$) and granzyme B (14.3% ± 0.6% vs.

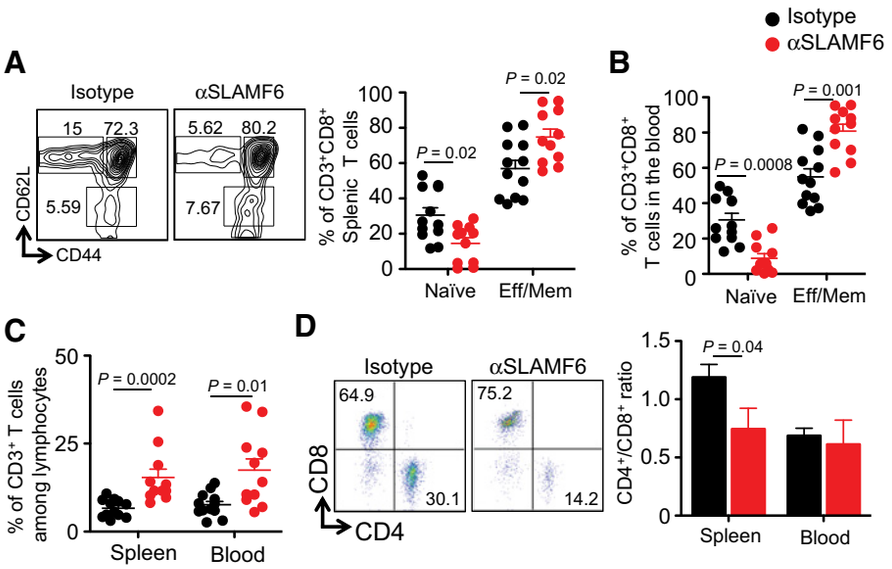

Figure 3.

Administering anti-SLAMF6 causes a skewing of $CD8^+$ T cells toward a memory phenotype in WT mice. Cells from isotype-injected ($n = 12$) or anti-SLAMF6–injected ($n = 11$) mice were stained for CD3, CD4, CD8, CD44, and CD62L. Dead cells were excluded as DAPI negative. **A,** Left, representative flow cytometry plots for $CD8^+$ T-cell subsets. Right, naïve ($CD62L^+CD44^-$) and effector/memory (Eff/Mem; $CD62L^-CD44^+$, $CD62L^+CD44^+$) subsets presented as a percentage of $CD3^+CD8^+$ T cells in the spleen of isotype- vs. anti-SLAMF6–injected mice. **B,** Naïve and effector/memory (Eff/Mem) subsets presented as a percentage of $CD3^+CD8^+$ T cells in blood. **C,** Percentage of $CD3^+$ T cells from the spleen and blood of anti-SLAMF6– or isotype-injected recipient mice. **D,** Left, representative flow cytometry plots for $CD4^+$ and $CD8^+$ T cells pregated on $CD3^+$ cells. Right, $CD4^+/CD8^+$ T-cell ratio in the spleen and blood between isotype- and anti-SLAMF6–injected groups. All graphs depict mean ± SD. *P* values are as shown. The data obtained in three independent experiments were pooled. The two-sided Mann–Whitney *U* test was used for statistical analysis.

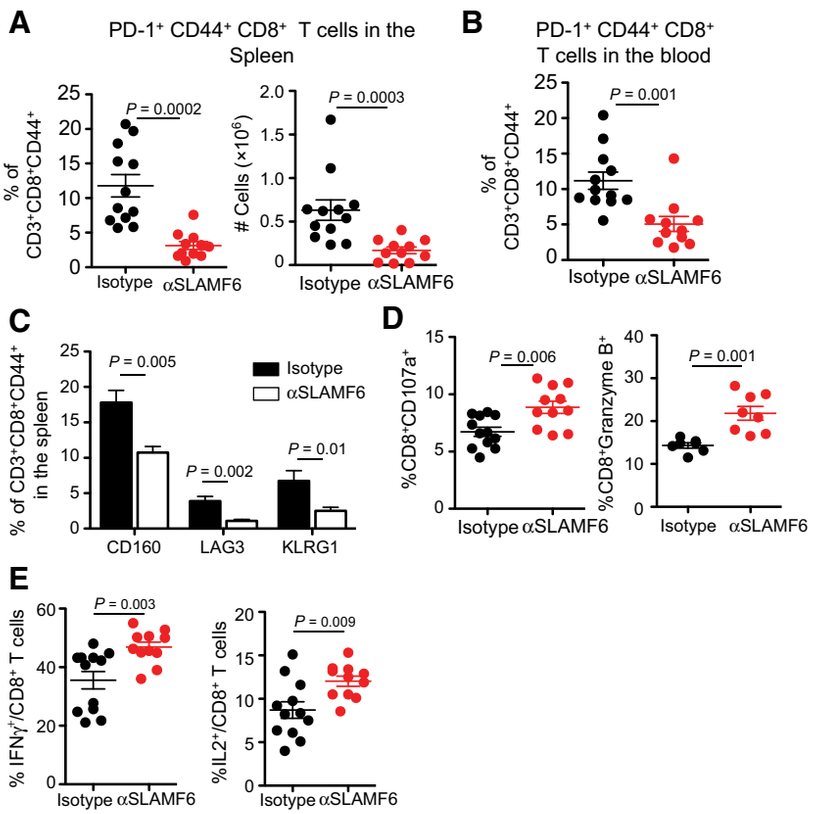

Figure 4.

In vivo administering of anti-SLAMF6 reduces the number of $PD1^+CD3^+CD44^+CD8^+$ T cells and improves effector functions. **A** and **B,** Percentage and absolute numbers of PD-1^+ antigen-experienced $CD8^+$ T cells ($CD3^+CD44^+CD8^+$) in the spleen (**A**) and blood (**B**) after administering isotype or anti-SLAMF6. **C,** Percentages of antigen-experienced $CD8^+$ T cells in the spleen expressing the exhaustion markers CD160, LAG3, and KLRG1 between anti-SLAMF6– and isotype-injected mice ($n = 5$/group). **D,** Freshly isolated total splenocytes from isotype- and anti-SLAMF6–injected mice were cultured with PMA/ionomycin for 4 hours in the presence of brefeldin A. After cell-surface staining with CD3 and CD8, cells were fixed and permeabilized for intracellular staining. CD107a antibody was added to the culture in the beginning. CD107a and granzyme B were a measure of cytotoxic capacity of $CD8^+$ T cells. **E,** IFNγ and IL2 as a measure of effector function of $CD8^+$ T cells in isotype vs. anti-SLAMF6 groups. The data obtained in three independent experiments were pooled (in **A**, **B**, **D**, and **E**). The two-sided Mann–Whitney *U* test was used for statistical analysis. All graphs depict mean ± SD. *P* values are as shown.

21.8% ± 1.5%, $P = 0.001$; Fig. 4D), and IFNγ-expressing (35.5% ± 2.9% vs. 46.8% ± 1.7%, $P = 0.003$) and IL2-expressing (8.7% ± 0.9% vs. 12% ± 0.5%, $P = 0.009$) $CD8^+$ T cells were significantly increased (Fig. 4E). From these data, we concluded that SLAMF6 is a negative checkpoint inhibitor, which restricts $CD8^+$ T-cell exhaustion in response to murine CLL cells. Consequently, signaling induced by anti-SLAMF6 reduced the number of exhausted $CD8^+$ T cells, which unleashes CTL responses against leukemic cells.

Reduction of TCL1 cells in the PerC of anti-SLAMF6–treated B6 mice

Previously, we have shown that anti-SLAMF6 fails to reduce the leukemic burden in the PerC of SCID mice into which the aggressive CLL clone TCL1-192 had been transferred (26). Upon administering anti-SLAMF6, a significantly reduced number of leukemic cells (3.1 ± 0.68 vs. 1.1 ± 0.26 × 10^7, $P = 0.01$), as well as a significantly reduced percentage of leukemic engraftment (91.4% ± 1.1% vs. 79.8% ± 2.7%, $P = 0.001$), was found in the PerC of WT recipients of Eμ-TCL1 cells (Fig. 5A). Similar to leukemic cells in spleen and blood, TCL1 cells residing in PerC of anti-SLAMF6–injected mice were significantly more proapoptotic compared with isotype-injected recipients (Fig. 5B).

Knowing that ADCC does not work in the PerC (30), we speculated that this reduction in leukemic engraftment might be due to activation of T cells. We found that the percentage of T cells had increased (1.5% ± 0.3% vs. 2.8% ± 0.4%, $P = 0.09$) and the $CD4^+/CD8^+$ ratio had decreased in anti-SLAMF6–injected mice compared with the control group, although it did not reach statistical significance (Fig. 5C). Although we did not find a change in $CD4^+$ T-cell subsets (Supplementary Fig. S4), we found a shift from naïve to eff/mem phenotype in $CD8^+$ T cells in the PerC of anti-SLAMF6–injected mice (naïve 38.7% ± 4.1% vs. 11.8% ± 2.04%, $P = 0.0004$; eff/mem 52.5 ± 4 vs. 75.8 ± 1.9, $P = 0.0009$; Fig. 5D). These activated $CD8^+$ T cells seen in the PerC with anti-SLAMF6 treatment led to increased frequency of PD-1 expression (percentage: 9.5 ± 1.1 vs. 3.6 ± 1.9, $P = 0.03$; absolute number: 1.7 ± 0.4 vs. 0.5 ± 0.3 × 10^4, $P = 0.09$; Fig. 5E). Because PD-1 expression can be correlated with either activation or exhaustion, it is plausible that the increase in PD-1^+CD8^+ T cells in the PerC may be a sign of activation at the time of analysis. In conclusion, as a single agent, anti-SLAMF6 reduced leukemic burden and engraftment not only in spleen, blood, and bone marrow but also in the PerC through activation of cytotoxic $CD8^+$ T cells.

Administering anti-SLAMF6 prevents expansion of B16 melanoma tumors

Although SLAMF6 expression is restricted to hematopoietic cells, we next asked whether anti-SLAMF6 could also empower the CTL response against nonhematopoietic tumors. To this end, we

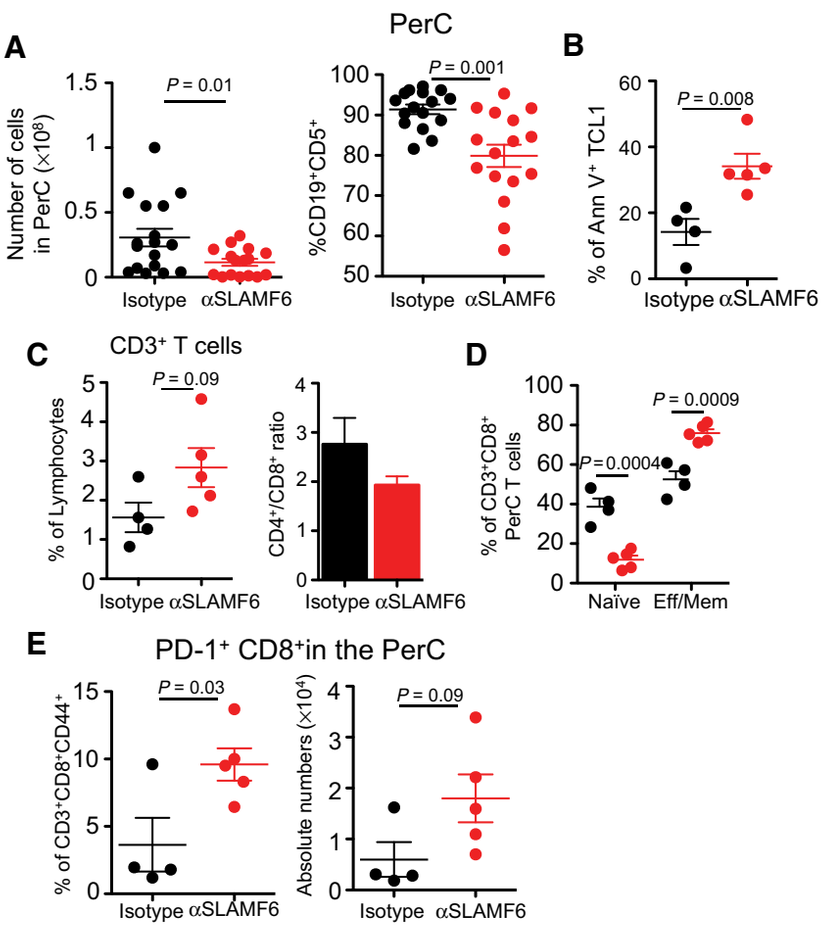

Figure 5.

Leukemic infiltration is reduced in the PerC of anti-SLAMF6–injected mice, along with an increase of activated $CD8^+$ T cells. **A,** The total number of cells and the percentage of $CD19^+CD5^+$ TCL1 cells isolated from the PerC in anti-SLAMF6–injected mice compared with the isotype-injected group. **B,** TCL1 cells isolated from the PerC of anti-SLAMF6–injected mice ($n = 5$) to compare apoptosis [percentage of Annexin V^+ ($AnnV^+$)] to TCL1 cells from isotype-injected mice ($n = 4$). **C,** Left, percentage of $CD3^+$ T cells from the PerC of anti-SLAMF6– or isotype-injected recipient mice. Right, $CD4^+/CD8^+$ T-cell ratio in the PerC compared between isotype- and anti-SLAMF6–injected groups. **D,** Naïve ($CD62L^+CD44^-$) and effector/memory (Eff/Mem; $CD62L^-CD44^+$, $CD62L^+CD44^+$) subsets presented as a percentage of $CD3^+CD8^+$ T cells in the PerC of isotype- vs. anti-SLAMF6–injected recipients. **E,** Percentage and absolute numbers of PD-1^+ antigen-experienced CD8 T cells ($CD3^+CD44^+CD8^+$) in the PerC. The unpaired Student *t* test was used for statistical analysis. All graphs depict mean ± SD. *P* values are as shown.

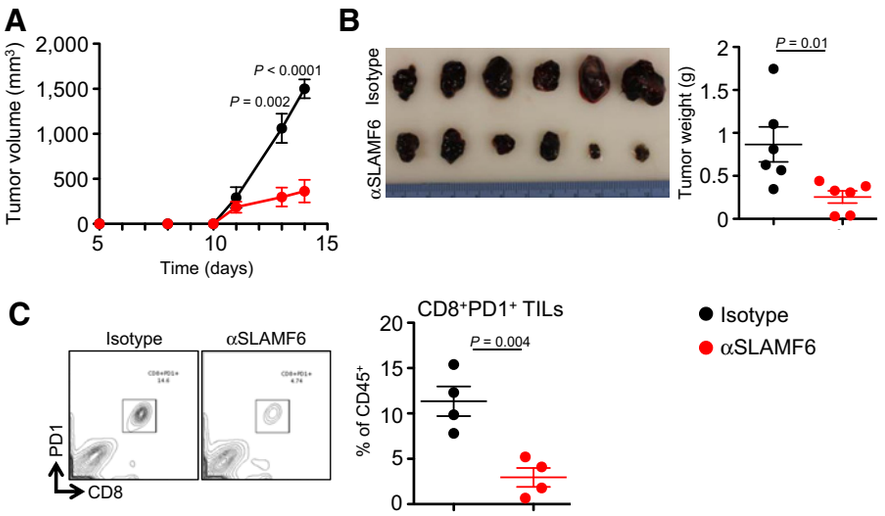

Figure 6.
One injection of anti-SLAMF6 reduces expansion of B16-OVA melanoma tumors. B16-OVA cells (10^5/mouse) were injected subcutaneously into B6 WT mice, and 8 days after tumor inoculation, when tumors were not yet palpable, mice were randomized and injected i.p. with 100 μg/mouse anti-SLAMF6 or isotype control. **A,** Tumor growth was monitored daily by measuring 3 diameters until day 15. **B,** Left, pictures of tumors harvested from anti-SLAMF6– or isotype-injected mice. Right, tumor weight. **C,** Isolated TILs were stained for CD45, CD8, and PD-1. Left, representative flow cytometry plots depicting $CD45^+CD8^+PD1^+$ T cells. Right, $CD8^+PD1^+$ T cells as a percentage of $CD45^+$ lymphocytes in the tumor. The data are representative of two independent experiments; unpaired Student *t* test was performed. All graphs depict mean ± SD. *P* values are as shown.

subcutaneously transplanted SLAMF6-negative B16 melanoma cells into B6 WT mice. Eight days after transplantation, mice were injected i.p. with 100 μg/mouse anti-SLAMF6 or isotype control. Tumor volume was monitored daily, and mice were euthanized on day 15 for analysis of tumor-infiltrating lymphocytes (TIL; Fig. 6A). As measured by solid tumor weight, mice injected with anti-SLAMF6 had significantly smaller tumors compared with isotype controls (0.8 ± 0.2 vs. 0.25 ± 0.07, $P = 0.01$; Fig. 6B). Upon analysis of $CD45^+$ lymphocytes in the tumor, we found significantly less percentages of $CD8^+$PD-1^+ TILs in anti-SLAMF6–injected mice compared with isotype control, suggesting activation of $CD8^+$ T cells in the tumor (11.3 ± 1.6 vs. 2.9 ± 1.03, $P = 0.004$; Fig. 6C). These findings suggest that anti-SLAMF6 is applicable not only to B-cell tumors but also to other cancer types.

Anti-human SLAMF6 increases degranulation of exhausted $CD8^+$ T cells

Next, we wanted to test whether our findings using anti-mouse SLAMF6 on exhausted $CD8^+$ T cells could also be observed using a human monoclonal antibody. To do this, we chronically stimulated PBMCs with anti-CD3/anti-CD28 three times and on day 8, generated exhausted $CD8^+$ T cells *in vitro* from healthy donors. Compared with freshly isolated PBMCs, we found significantly increased $CD8^+PD1^+$ T cells with chronic stimulation (Fig. 7A). We then checked the effect of mouse anti-human SLAMF6 (mαhSLAMF6) on the degranulation capacity of fresh and exhausted $CD8^+$ T cells. Cells were stimulated *in vitro* with anti-CD3 and anti-CD28 along with isotype or anti-hSLAMF6 for 4 hours, and degranulation was measured by CD107a staining. Comparing fresh and exhausted $CD8^+$ T cells receiving isotype antibody showed significantly reduced degranulation capacity in exhausted $CD8^+$ T cells compared with fresh cells (Fig. 7B, left). Although mαhSLAMF6 had no effect on the degranulation of fresh $CD8^+$ T cells, it significantly increased degranulation of exhausted $CD8^+$ T cells (Fig. 7B, middle and right). This suggested that signaling through SLAMF6 may be altered in exhausted T cells and could be reversed using a monoclonal antibody.

Anti-human SLAMF6 affects $CD8^+$ T cells from CLL patients

To begin to translate our results for therapeutic purposes, we set up *in vitro* experiments with a humanized anti-human SLAMF6 (αhSLAMF6). First, we tested the capacity of the antibody on $CD8^+$ T cells of CLL patients. When T cells were stimulated *in vitro* with anti-CD3/anti-CD28 in the presence of isotype or αhSLAMF6 for 4 hours, $CD8^+$ T cells had significantly increased degranulation capacity with αhSLAMF6 treatment, as judged by CD107a staining (Fig. 7C). Degranulation from $CD8^+$ T cells of CLL patients was comparable to that of exhausted T cells generated *in vitro* from healthy donors (Fig. 7A and B), suggesting that exhausted $CD8^+$ T cells could be activated through a SLAMF6 signaling–related mechanism. This also demonstrated that the effect of anti-human SLAMF6 appears to be comparable irrespective of the Fc being mouse or human.

Because we know that SLAMF6 has an effect on BCR signaling, we determined the viability of human CLL cells with αhSLAMF6 in the presence of and in combination with ibrutinib. We used PBMCs from IGHV-unmutated CLL patients with varying levels of IgM surface expression (Supplementary Table S1). Ibrutinib alone served as a positive control for the system, as its interference with BCR-induced survival *in vitro* is well established (31). CLL cells were either stimulated with anti-human IgM or left unstimulated, and ibrutinib, anti-hSLAMF6, or both were added to the cells. CLL viability was determined as a percentage of Annexin V/PI-negative cells 24 or 48 hours after stimulation (Fig. 7D). We found that upon BCR stimulation, the addition of anti-hSLAMF6 alone reduced viability to comparable levels as those of ibrutinib, and this was enhanced if the two were combined, suggesting that the improved effect of combining anti-SLAMF6 and ibrutinib we observed *in vivo* also applies to human CLL cells in an *in vitro* setting.

Discussion

Overcoming immune evasion, a phenomenon by which pathogens and cancer cells escape the host immune system, is being actively pursued to identify immune checkpoints for therapeutic targeting. Chief among the successfully exploited mechanisms is

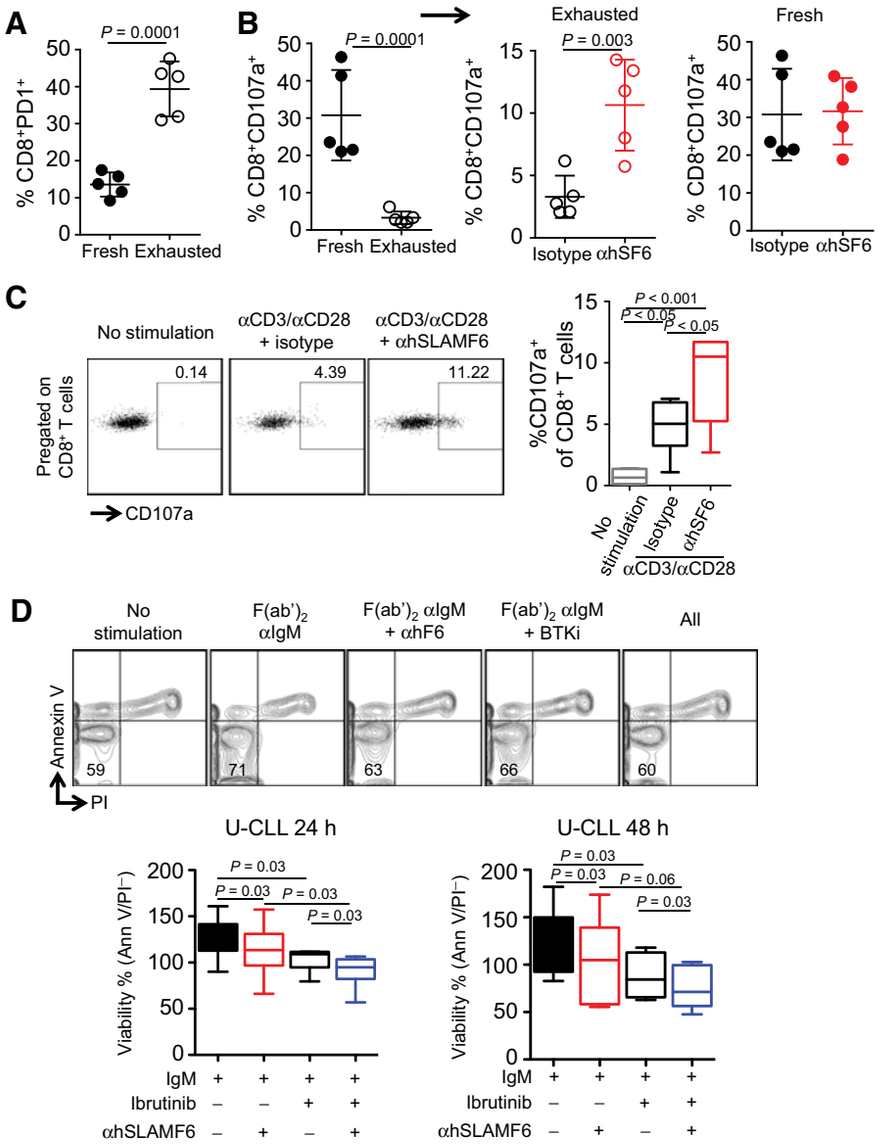

Figure 7.

Anti-human SLAMF6 increases degranulation of exhausted CD8$^+$ T cells and reduces BCR signaling–mediated viability of CLL cells. Fresh PBMCs were obtained from healthy donors ($n = 5$). Cells were stimulated with plate-bound anti-CD3/anti-CD28 (1 mg/mL each). Every 2 days, cells were washed and transferred to a new plate with the same conditions for 8 days. **A,** Day 8 comparison of exhaustion, measured by PD-1$^+$ on CD8$^+$ T cells, from cells unstimulated or chronically stimulated (fresh vs. exhaustion, respectively). **B,** Left, day 8 comparison of degranulation capacity of fresh and exhausted CD8$^+$ T cells. Right, fresh, or, middle, exhausted CD8$^+$ T cells stimulated with isotype or anti-hSLAMF6. **C,** T cells from CLL patients ($n = 5$) were cultured in the presence of plate-bound anti-CD3/anti-CD28 (5 μg/mL each) along with anti-hSLAMF6 (5 μg/mL) or isotype control (mouse IgG2b) for 4 hours. CD107a was added to the cultures from the beginning. Cells were then stained for CD8 to measure degranulation. Left, representative flow cytometry plots for CD107a. Right, percentage of CD107a$^+$CD8$^+$ T cells under no stimulation or stimulation with anti-SLAMF6 or isotype control. **D,** PBMCs from IGHV-unmutated CLL patients ($n = 6$) were cultured in the presence of anti-human F(ab′)$_2$ IgM, ibrutinib (BTKi, BTK inhibitor), and anti-hSLAMF6 or in combination for 24 and 48 hours (h). Viability of cells was measured by Annexin V/PI staining. Representative gating is as shown. Viability of unstimulated wells was set to 100% as a baseline, and percentage of viability was calculated accordingly. Data are pooled from two independent experiments. For statistical analyses, nonparametric Wilcoxon signed-rank test was used. All graphs depict mean ± SD. *P* values are as shown.

the well-characterized PD-1/PD-L1 axis. Blockade of this pathway has proven to be effective in solid tumors, as well as hematologic malignancies (8, 9).

CLL is well known to generate impaired immune responses in the host, with the malignant clone residing in well-vascularized tissues and circulating in peripheral blood but also in close proximity to effector cells that are capable, if activated appropriately, of carrying out a cytotoxic response. Defective T-cell responses have been observed in CLL patients, including imbalance of T-cell subsets, inability to form immune synapses between CLL B cells and T cells, increased expression of inhibitory receptors (e.g., PD-1, CD160, and LAG3), and loss in proliferation and cytotoxic capacity (2, 3, 7, 32, 33). These, in turn, result in ineffective antitumor responses. Thus, treatment protocols are based on agents with the ability to generate an immune response, e.g., anti-CD20, checkpoint inhibitors, or cellular therapies (34).

Currently, the most effective method of studying the tumor microenvironment is through the use of murine models (35). In this study, we used the Eμ-TCL1 adoptive transfer model to assess the relevance of SLAMF6 in the murine CLL microenvironment and the usefulness of targeting this receptor with a monoclonal antibody to SLAMF6 to improve its therapeutic action on leukemic cell expansion and enhance CD8$^+$ T-cell functions. When Eμ-TCL1 leukemic cells were made to reside in a tumor microenvironment that lacks SLAMF6, i.e., the SLAMF6$^{-/-}$ mouse, we observed an expansion of a PD-1$^+$ subset of CD3$^+$CD44$^+$CD8$^+$ T cells with reduced cytotoxic functions. This supports the concept that SLAMF6–SLAMF6 interactions, and possibly intracellular signaling initiated from this interaction, are important in the development of CD8$^+$ T-cell functions.

This concept was further supported by the outcomes of our experiments with anti-SLAMF6, which *in vivo* reduced the leukemic burden in the Eμ-TCL1 adoptive transfer model.

Administering anti-SLAMF6 reduced the number and proportion of $PD1^+CD3^+CD44^+CD8^+$ T cells concomitantly with an increase in cytotoxicity, as determined by expression of CD107a and granzyme B. Possible reasons for reduction in exhausted $PD1^+CD8^+$ T cells include induction of ADCC and/or downregulation of PD-1 from the cell surface after SLAMF6 ligation. SLAMF6 serves as a costimulatory receptor in T cells and recruits SAP to its cytoplasmic tail. We found no effect of SAP deficiency in this system when murine CLL cells were transferred into $SAP^{-/-}$ mice. This suggests that our findings are independent of SAP, but whether there is a direct link between SLAMF6 and PD-1 signaling needs further investigation.

The change in the $CD4^+/CD8^+$ T-cell ratio appears to be associated with CLL progression (1, 5, 36, 37). This association is complemented by the findings that both $CD4^+$ and $CD8^+$ T cells acquire a PD-1^+ phenotype that is associated with their inability to perform effector functions (5, 7, 36–38). Although the shift in the $CD4^+/CD8^+$ ratio appeared to be inverted in our system, anti-SLAMF6 was able to restore the phenotype and functions of exhausted $CD8^+$ T cells, which would support the notion that exhausted T cells need to be reactivated within the suppressive tumor microenvironment for antitumor immunity. Thus, empowering $CD8^+$ T-cell effector functions adds to the ability of anti-SLAMF6 to control disease by removing the CLL cells by ADCC and downregulating BCR signaling.

This dual activity of anti-SLAMF6 is in contrast with the mechanism by which anti-CD20 and ibrutinib control CLL in patients (34) Primarily, anti-SLAMF6 induces activation of ADCC mediated by engagement of antibody Fc portion with Fc receptors on macrophages and NK cells (26). Secondly, signaling of SLAMF6 in CLL B cells reduces proximal BCR signaling and survival in both murine and human models. Lastly, antibody binding to SLAMF6 on the surface of T cells causes reduction in the number of PD-$1^+CD3^+CD44^+CD8^+$ T cells and results in increased effector functions of remaining $CD8^+$ T cells. This finding of the anti-SLAMF6 applies to other models as well. Previously, our lab demonstrated that injections of anti-SLAMF6 inhibit antibody responses in an immunization model (24). Inhibition of antibody production coincides with our finding that anti-SLAMF6 reduced BCR signaling, thus survival of B cells. We also found that i.p. injection of anti-SLAMF6 to subcutaneously growing B16 melanoma cells significantly reduced the tumor growth. Because melanoma cells do not express SLAMF6, this was through the reduction in the percentage of $PD1^+CD8^+$ T cells that infiltrated the tumor, suggesting activation of T-cell responses. This suggests that there is a selection by the antibody toward the PD-1^+ subpopulation in activated $CD8^+$ T cells, and this was irrespective of the disease model used.

To confirm the relevance of our findings in the mouse models, we used both CLL $CD8^+$ T cells as well as generated exhausted $CD8^+$ T cells *in vitro* and demonstrated that anti-human SLAMF6 increased degranulation of these exhausted cells. In these short cultures, it was not possible to dissect the effect of antibody on numbers of exhausted $CD8^+$ T cells. It was previously shown that SLAMF6 partakes in restimulation-induced cell death (RICD) involving interactions through SAP and LCK (39). It is also possible to think that anti-SLAMF6 and anti-hSLAMF6 induced RICD in exhausted $CD8^+$ T cells in our models.

Recently, Ayers and colleagues (40) identified IFNγ-related gene-expression profiles that could predict response to PD-1 checkpoint blockade in a variety of tumor types. Starting with 19 and validating in 62 melanoma patients, a "preliminary expanded immune" 28-gene set correlating with IFNγ signatures was identified. One of these genes was SLAMF6. IFNγ signaling is known to associate with a T cell–inflamed microenvironment that responds to anti–PD-1 therapy. This may be a platform to test combination of anti-SLAMF6 together with anti–PD-1 for a better T-cell response against various tumors.

We found that the leukemic burden and infiltration of Eμ-TCL1 cells in the PerC was lowered by anti-SLAMF6. Leukemic cells, as well normal B cells, show different characteristics when they are in the PerC or in the spleen, and one idea is that the PerC is a hypoxic niche that favors adhesion and growth of tumors (41–44). We previously demonstrated no ADCC effect of anti-SLAMF6 in PerC in a T cell–independent system, similar to that observed with anti-CD20 injections (26, 30). Although the ADCC function of an antibody is eliminated in this niche due to the microenvironment, signaling through SLAMF6 in T cells was able to reduce tumor infiltration. Anti-SLAMF6 was selectively targeting PD-$1^+CD3^+CD44^+CD8^+$ T cells in the spleen and blood and possibly induced their killing by ADCC. However, because the antibody was unable to induce ADCC in the PerC, it enriched for $PD1^+CD8^+$ T cells. This suggests that there is a correlation between PD-1 and SLAMF6 signaling, and understanding the mechanisms behind this may be relevant therapeutically. PD-1 contains a cytoplasmic tail with an ITSM that binds SHP1 and SHP2, similar to that in SLAMF6 (45–47). There may be a competition for binding of SHP1/2 that, in turn, dictates the responses from T cells. Understanding these niche-dependent changes to tumor killing is important, as there may be niches in the human body that are not accessible for certain type of treatments.

Peritoneal metastases of ovarian, pancreatic, gastric, and colon cancers are common, and in most cases, are of poor prognosis and survival rate if left untreated (48–51). Targeting and treatment of peritoneal tumors remain a challenge due to delivery, pharmacology, and efficacy (51). Regional chimeric antigen receptor (CAR) T-cell infusion for peritoneal carcinomatosis has shown to be effective, suggesting that the regional activation of T cells is important in clearing of tumors in the peritoneum (52, 53). It would be of interest to test in different models of peritoneal tumors whether targeting SLAMF6 could play a role in clearing these tumors.

Overall, besides the ability of anti-SLAMF6 to induce ADCC, improvement in effector $CD8^+$ T-cell responses makes SLAMF6 an intriguing candidate for therapy, as it appears to work not only on tumors in secondary lymphoid organs and the peripheral blood but also in hypoxic niches such as the PerC or in solid tumors. We propose that anti-SLAMF6 alone or in combination should be further explored in B-cell leukemias and lymphomas in a clinical setting.

Disclosure of Potential Conflicts of Interest

No potential conflicts of interest were disclosed.

Authors' Contributions

Conception and design: B. Yigit, N. Wang, E. ten Hacken, A. Suarez-Fueyo, J.A. Burger, R.W. Herzog, P. Engel, C. Terhorst

Development of methodology: B. Yigit, N. Wang, A. Suarez-Fueyo, N. Chiorazzi, R.W. Herzog, P. Engel
Acquisition of data (provided animals, acquired and managed patients, provided facilities, etc.): B. Yigit, N. Wang, E. ten Hacken, A.K. Bhan, A. Suarez-Fueyo, E. Katsuyama, N. Chiorazzi, C. Terhorst
Analysis and interpretation of data (e.g., statistical analysis, biostatistics, computational analysis): B. Yigit, N. Wang, E. ten Hacken, A. Suarez-Fueyo, E. Katsuyama, G.C. Tsokos, C.J. Wu, J.A. Burger, C. Terhorst
Writing, review, and/or revision of the manuscript: B. Yigit, N. Wang, E. ten Hacken, A. Suarez-Fueyo, G.C. Tsokos, C.J. Wu, J.A. Burger, C. Terhorst
Administrative, technical, or material support (i.e., reporting or organizing data, constructing databases): B. Yigit, S.-S. Chen
Study supervision: B. Yigit, C. Terhorst

Acknowledgments

This work was supported by grants from the NIH PO1-AI065687 to C. Terhorst, N. Wang, and P. Engel. A. Suarez-Fueyo was supported by AI074549 (to G.C. Tsokos). E. ten Hacken is a Special Fellow of the Leukemia & Lymphoma Society.

The costs of publication of this article were defrayed in part by the payment of page charges. This article must therefore be hereby marked *advertisement* in accordance with 18 U.S.C. Section 1734 solely to indicate this fact.

Received September 19, 2018; revised February 28, 2019; accepted July 10, 2019; published first July 17, 2019.

References

1. Gorgun G, Holderried TA, Zahrieh D, Neuberg D, Gribben JG. Chronic lymphocytic leukemia cells induce changes in gene expression of CD4 and CD8 T cells. J Clin Invest 2005;115:1797–805.
2. Ramsay AG, Johnson AJ, Lee AM, Gorgun G, Le Dieu R, Blum W, et al. Chronic lymphocytic leukemia T cells show impaired immunological synapse formation that can be reversed with an immunomodulating drug. J Clin Invest 2008;118:2427–37.
3. Riches JC, Davies JK, McClanahan F, Fatah R, Iqbal S, Agrawal S, et al. T cells from CLL patients exhibit features of T-cell exhaustion but retain capacity for cytokine production. Blood 2013;121:1612–21.
4. Brusa D, Serra S, Coscia M, Rossi D, D'Arena G, Laurenti L, et al. The PD-1/PD-L1 axis contributes to T-cell dysfunction in chronic lymphocytic leukemia. Haematologica 2013;98:953–63.
5. Nunes C, Wong R, Mason M, Fegan C, Man S, Pepper C. Expansion of a CD8(+)PD-1(+) replicative senescence phenotype in early stage CLL patients is associated with inverted CD4:CD8 ratios and disease progression. Clin Cancer Res 2012;18:678–87.
6. Wherry EJ. T cell exhaustion. Nat Immunol 2011;12:492–9.
7. Zenz T. Exhausting T cells in CLL. Blood 2013;121:1485–6.
8. Topalian SL, Hodi FS, Brahmer JR, Gettinger SN, Smith DC, McDermott DF, et al. Safety, activity, and immune correlates of anti-PD-1 antibody in cancer. N Engl J Med 2012;366:2443–54.
9. Xu-Monette ZY, Zhou J, Young KH. PD-1 expression and clinical PD-1 blockade in B-cell lymphomas. Blood 2018;131:68–83.
10. Peck SR, Ruley HE. Ly108: a new member of the mouse CD2 family of cell surface proteins. Immunogenetics 2000;52:63–72.
11. Cao E, Ramagopal UA, Fedorov A, Fedorov E, Yan Q, Lary JW, et al. NTB-A receptor crystal structure: insights into homophilic interactions in the signaling lymphocytic activation molecule receptor family. Immunity 2006;25:559–70.
12. Fraser CC, Howie D, Morra M, Qiu Y, Murphy C, Shen Q, et al. Identification and characterization of SF2000 and SF2001, two new members of the immune receptor SLAM/CD2 family. Immunogenetics 2002;53:843–50.
13. Bottino C, Falco M, Parolini S, Marcenaro E, Augugliaro R, Sivori S, et al. NTB-A [correction of GNTB-A], a novel SH2D1A-associated surface molecule contributing to the inability of natural killer cells to kill Epstein-Barr virus-infected B cells in X-linked lymphoproliferative disease. J Exp Med 2001;194:235–46.
14. Eissmann P, Watzl C. Molecular analysis of NTB-A signaling: a role for EAT-2 in NTB-A-mediated activation of human NK cells. J Immunol 2006;177:3170–7.
15. Flaig RM, Stark S, Watzl C. Cutting edge: NTB-A activates NK cells via homophilic interaction. J Immunol 2004;172:6524–7.
16. Griewank K, Borowski C, Rietdijk S, Wang N, Julien A, Wei DG, et al. Homotypic interactions mediated by Slamf1 and Slamf6 receptors control NKT cell lineage development. Immunity 2007;27:751–62.
17. Howie D, Laroux FS, Morra M, Satoskar AR, Rosas LE, Faubion WA, et al. Cutting edge: the SLAM family receptor Ly108 controls T cell and neutrophil functions. J Immunol 2005;174:5931–5.
18. Wang N, Halibozek PJ, Yigit B, Zhao H, O'Keeffe MS, Sage P, et al. Negative regulation of humoral immunity due to interplay between the SLAMF1, SLAMF5, and SLAMF6 receptors. Front Immunol 2015;6:158.
19. De Calisto J, Wang N, Wang G, Yigit B, Engel P, Terhorst C. SAP-dependent and -independent regulation of innate T cell development involving SLAMF receptors. Front Immunol 2014;5:186.
20. Chan B, Lanyi A, Song HK, Griesbach J, Simarro-Grande M, Poy F, et al. SAP couples Fyn to SLAM immune receptors. Nat Cell Biol 2003;5:155–60.
21. Calpe S, Wang N, Romero X, Berger SB, Lanyi A, Engel P, et al. The SLAM and SAP gene families control innate and adaptive immune responses. Adv Immunol 2008;97:177–250.
22. Kageyama R, Cannons JL, Zhao F, Yusuf I, Lao C, Locci M, et al. The receptor Ly108 functions as a SAP adaptor-dependent on-off switch for T cell help to B cells and NKT cell development. Immunity 2012;36:986–1002.
23. Zhao F, Cannons JL, Dutta M, Griffiths GM, Schwartzberg PL. Positive and negative signaling through SLAM receptors regulate synapse organization and thresholds of cytolysis. Immunity 2012;36:1003–16.
24. Wang N, Keszei M, Halibozek P, Yigit B, Engel P, Terhorst C. Slamf6 negatively regulates autoimmunity. Clin Immunol 2016;173:19–26.
25. Chen SS, Batliwalla F, Holodick NE, Yan XJ, Yancopoulos S, Croce CM, et al. Autoantigen can promote progression to a more aggressive TCL1 leukemia by selecting variants with enhanced B-cell receptor signaling. PNAS 2013;110:E1500–7.
26. Yigit B, Halibozek PJ, Chen SS, O'Keeffe MS, Arnason J, Avigan D, et al. A combination of an anti-SLAMF6 antibody and ibrutinib efficiently abrogates expansion of chronic lymphocytic leukemia cells. Oncotarget 2016;7:26346–60.
27. Keszei M, Detre C, Rietdijk ST, Munoz P, Romero X, Berger SB, et al. A novel isoform of the Ly108 gene ameliorates murine lupus. J Exp Med 2011;208:811–22.
28. Wu C, Nguyen KB, Pien GC, Wang N, Gullo C, Howie D, et al. SAP controls T cell responses to virus and terminal differentiation of TH2 cells. Nat Immunol 2001;2:410–4.
29. Fankhauser M, Broggi MAS, Potin L, Bordry N, Jeanbart L, Lund AW, et al. Tumor lymphangiogenesis promotes T cell infiltration and potentiates immunotherapy in melanoma. Sci Transl Med 2017;9. pii:eaal4712.
30. Hamaguchi Y, Uchida J, Cain DW, Venturi GM, Poe JC, Haas KM, et al. The peritoneal cavity provides a protective niche for B1 and conventional B lymphocytes during anti-CD20 immunotherapy in mice. J Immunol 2005;174:4389–99.
31. Ponader S, Chen SS, Buggy JJ, Balakrishnan K, Gandhi V, Wierda WG, et al. The Bruton tyrosine kinase inhibitor PCI-32765 thwarts chronic lymphocytic leukemia cell survival and tissue homing in vitro and in vivo. Blood 2012;119:1182–9.
32. Riches JC, Ramsay AG, Gribben JG. T-cell function in chronic lymphocytic leukaemia. Semin Cancer Biol 2010;20:431–8.
33. Ramsay AG, Clear AJ, Fatah R, Gribben JG. Multiple inhibitory ligands induce impaired T-cell immunologic synapse function in chronic lymphocytic leukemia that can be blocked with lenalidomide: establishing a reversible immune evasion mechanism in human cancer. Blood 2012;120:1412–21.
34. Freeman CL, Gribben JG. Immunotherapy in Chronic Lymphocytic Leukaemia (CLL). Curr Hematol Malig Rep 2016;11:29–36.

35. Bichi R, Shinton SA, Martin ES, Koval A, Calin GA, Cesari R, et al. Human chronic lymphocytic leukemia modeled in mouse by targeted TCL1 (26) expression. PNAS 2002;99:6955–60.
36. Gonzalez-Rodriguez AP, Contesti J, Huergo-Zapico L, Lopez-Soto A, Fernandez-Guizan A, Acebes-Huerta A, et al. Prognostic significance of CD8 and CD4 T cells in chronic lymphocytic leukemia. Leuk Lymphoma 2010;51:1829–36.
37. Gothert JR, Eisele L, Klein-Hitpass L, Weber S, Zesewitz ML, Sellmann L, et al. Expanded CD8+ T cells of murine and human CLL are driven into a senescent KLRG1+ effector memory phenotype. Cancer Immunol Immunother 2013;62:1697–709.
38. Scrivener S, Goddard RV, Kaminski ER, Prentice AG. Abnormal T-cell function in B-cell chronic lymphocytic leukaemia. Leuk Lymphoma 2003;44:383–9.
39. Katz G, Krummey SM, Larsen SE, Stinson JR, Snow AL. SAP facilitates recruitment and activation of LCK at NTB-A receptors during restimulation-induced cell death. J Immunol 2014;192:4202–9.
40. Ayers M, Lunceford J, Nebozhyn M, Murphy E, Loboda A, Kaufman DR, et al. IFN-gamma-related mRNA profile predicts clinical response to PD-1 blockade. J Clin Invest 2017;127:2930–40.
41. Miao ZF, Wang ZN, Zhao TT, Xu YY, Gao J, Miao F, et al. Peritoneal milky spots serve as a hypoxic niche and favor gastric cancer stem/progenitor cell peritoneal dissemination through hypoxia-inducible factor 1alpha. Stem Cells 2014;32:3062–74.
42. Noda S, Yashiro M, Nshii T, Hirakawa K. Hypoxia upregulates adhesion ability to peritoneum through a transforming growth factor-beta-dependent mechanism in diffuse-type gastric cancer cells. Eur J Cancer 2010;46:995–1005.
43. Tumang JR, Hastings WD, Bai C, Rothstein TL. Peritoneal and splenic B-1 cells are separable by phenotypic, functional, and transcriptomic characteristics. Eur J Immunol 2004;34:2158–67.
44. Yigit B, Wang N, Chen SS, Chiorazzi N, Terhorst C. Inhibition of reactive oxygen species limits expansion of chronic lymphocytic leukemia cells. Leukemia 2017;31:2273–6.
45. Carter L, Fouser LA, Jussif J, Fitz L, Deng B, Wood CR, et al. PD-1:PD-L inhibitory pathway affects both CD4(+) and CD8(+) T cells and is overcome by IL-2. Eur J Immunol 2002;32:634–43.
46. Yokosuka T, Takamatsu M, Kobayashi-Imanishi W, Hashimoto-Tane A, Azuma M, Saito T. Programmed cell death 1 forms negative costimulatory microclusters that directly inhibit T cell receptor signaling by recruiting phosphatase SHP2. J Exp Med 2012;209:1201–17.
47. Bardhan K, Anagnostou T, Boussiotis VA. The PD1:PD-L1/2 pathway from discovery to clinical implementation. Front Immunol 2016;7:550.
48. Dahdaleh FS, Turaga KK. Evolving treatment strategies and outcomes in advanced gastric cancer with peritoneal metastasis. Surg Oncol Clin N Am 2018;27:519–37.
49. Carlomagno C, De Stefano A, Rosanova M, De Falco S, Attademo L, Fiore G, et al. Multiple treatment lines and prognosis in metastatic colorectal cancer patients. Cancer Metastasis Rev 2019;38:307–13.
50. Ghoneum A, Afify H, Salih Z, Kelly M, Said N. Role of tumor microenvironment in the pathobiology of ovarian cancer: insights and therapeutic opportunities. Cancer Med 2018;7:5047–56.
51. Reha J, Katz SC. Regional immunotherapy for liver and peritoneal metastases. J Surg Oncol 2017;116:46–54.
52. Ang WX, Li Z, Chi Z, Du SH, Chen C, Tay JC, et al. Intraperitoneal immunotherapy with T cells stably and transiently expressing anti-EpCAM CAR in xenograft models of peritoneal carcinomatosis. Oncotarget 2017;8:13545–59.
53. Katz SC, Point GR, Cunetta M, Thorn M, Guha P, Espat NJ, et al. Regional CAR-T cell infusions for peritoneal carcinomatosis are superior to systemic delivery. Cancer Gene Ther 2016;23:142–8.